High-Fidelity Rapid Initialization and Read-Out of an Electron Spin via the Single Donor D^{-} Charge State

T. F. Watson, B. Weber, M. G. House, H. Büch, and M. Y. Simmons

Phys. Rev. Lett. **115**, 166806 — Published 16 October 2015

DOI: 10.1103/PhysRevLett.115.166806

High-fidelity rapid initialisation and readout of an electron spin via the single donor D^- charge state

T. F. Watson,[1] B. Weber,[1,*] M. G. House,[1] H. Büch,[1,†] and M. Y. Simmons[1,‡]

[1] *Australian Research Council Centre of Excellence for Quantum Computation and Communication Technology, University of New South Wales, Sydney, NSW 2052, Australia*

(Dated: September 22, 2015)

We demonstrate high-fidelity electron spin readout of a precision placed single donor in silicon via spin selective tunnelling to either the D^+ or D^- charge state of the donor. By performing readout at the stable two electron $D^0 \leftrightarrow D^-$ charge transition we can increase the tunnel rates to a nearby SET charge sensor by nearly two orders of magnitude, allowing faster qubit readout (1 ms) with minimum loss in readout fidelity (98.4%) compared to readout at the $D^+ \leftrightarrow D^0$ transition (99.6%). Furthermore, we show that readout via the D^- charge state can be used to rapidly initialise the electron spin qubit in its ground state with a fidelity of $F_I = 99.8\%$.

Electron spins confined in solids are attractive qubits due to long coherence times [1, 2], fast gate operations [3, 4] and potential for scalability [5, 6]. Particularly donor-bound spins in silicon show coherence times of milliseconds with the ability to store quantum information in the donor nuclei [1, 7, 8]. Initialisation and readout has been achieved via spin selective tunnelling to an electron reservoir [9, 10] with fidelities as high as 97% [1, 2, 11, 12]. However, robust quantum error correction protocols such as the surface code require fidelities of $\sim 99\%$ with the measurement of parity operators to detect and correct errors faster than qubit coherence times [13, 14]. Readout times and fidelity can be optimised by tuning electron tunnel rates to the reservoir [9]. This can however be challenging in donors [15–17] due to their close proximity to the reservoir and the stochastic nature of doping in many device architectures [10, 18, 19]. Here we demonstrate that we can decrease the readout times of a single phosphorus donor by nearly two orders of magnitude to 1 ms by selecting the two-electron D^- state in a novel pulse sequence. Importantly, we observe no significant loss in qubit readout fidelity (98.4%), compared to a record fidelity of 99.6% obtained using conventional readout, giving the highest fidelity for such rapid spin readout [1, 2]. Both readout schemes can be used to rapidly initialize spins with fidelities $F_I \geq 99.8\%$.

An overview of the device after STM hydrogen lithography [20] is shown in Fig. 1(a). Details of the device fabrication process have been published previously [16, 21, 22]. The device hosts two donor sites, D1 and D2, placed 25 nm apart at a distance ~ 20 nm from a single electron transistor (SET) [11] which acts as charge sensor and electron reservoir [10]. Following lithography, this device template was selectively doped with PH_3 followed by annealing (350 °C) providing an atomically abrupt planar doping profile with density $N_{2D} \approx 2 \times 10^{18}$ m^{-2}) [23]. We estimate a maximum of two donors to be incorporated in D1 and D2 from the STM images in Fig. 1(b-c), respectively [16, 24]. Charge sensing measurements show that a single donor was incorporated in D2 while no donor was incorporated in D1 (see Supplemental Material S1 [25]). Four in-plane gates, G1, G2, GSET, and GT, are used to tune the electrochemical potentials of the donor and SET island. All experiments were performed at low temperature with a measured electron temperature of $T_e \sim 160$ mK (see Supplemental Material S2).

The charge stability diagram, recorded at $V_{SD} = 0.75$ mV and $V_{GT} = V_{GSET} = 1$ V, is plotted in Fig. 1(d), showing the SET current as a function of the gate voltages V_{G1} and V_{G2}. Lines of current running at $\sim 45°$ correspond to the Coulomb blockade (CB) peaks of the SET whenever its electrochemical potential is aligned between the Fermi level of the source and drain electrodes. Charge transitions on the donor are detected by shifts of the electrochemical potential of the SET [10, 26], resulting in two parallel lines of charge offsets in the CB pattern (white dotted lines). The presence of two sets of charge transitions is consistent with a single P donor which can bind up to two electrons [27] within three stable charge states, D^+ (0e), D^0 (1e), and D^- (2e). From the separation of the $D^+ \leftrightarrow D^0$ and $D^0 \leftrightarrow D^-$ transitions in gate space we extract a charging energy, $E_C = 50 \pm 7$ meV, in good agreement with that of bulk P donors [27] and an STM-patterned single-atom transistor [24]. The horizontal offset marked by the red arrow in Fig. 1(d) is due to a trapped charge rearrangement.

The energy level diagram of a single donor with ground and excited states for both the D^0 and D^- charge states is shown in Fig. 1(e) [28]. A static magnetic field, B, splits the spin-degenerate D^0 ground state into spin up $|\uparrow\rangle$ and spin down $|\downarrow\rangle$, separated by the Zeeman energy, $\Delta E_Z = g\mu_B B$. The resulting electrochemical potentials $\mu_{0\leftrightarrow\downarrow}$ and $\mu_{0\leftrightarrow\uparrow}$ (coloured arrows) allow spin readout at the $D^+ \leftrightarrow D^0$ charge transition (blue box in Fig. 1(d)) [10, 11] by applying a three level pulse sequence as shown in the left hand panel of Fig 2. For readout both electrochemical potentials are aligned such that $\mu_{0\leftrightarrow\downarrow}$ is below and $\mu_{0\leftrightarrow\uparrow}$ is above the electrochemical potential of the SET allowing spin-selective tunnelling to the SET island. If the electron spin is in the $|\uparrow\rangle$ state then it will tunnel onto the SET island, followed by a $|\downarrow\rangle$ returning to the donor resulting in a single pulse in the SET current (blue trace in Fig 2(b)). The time scale for readout at this transition can be extracted from histograms of

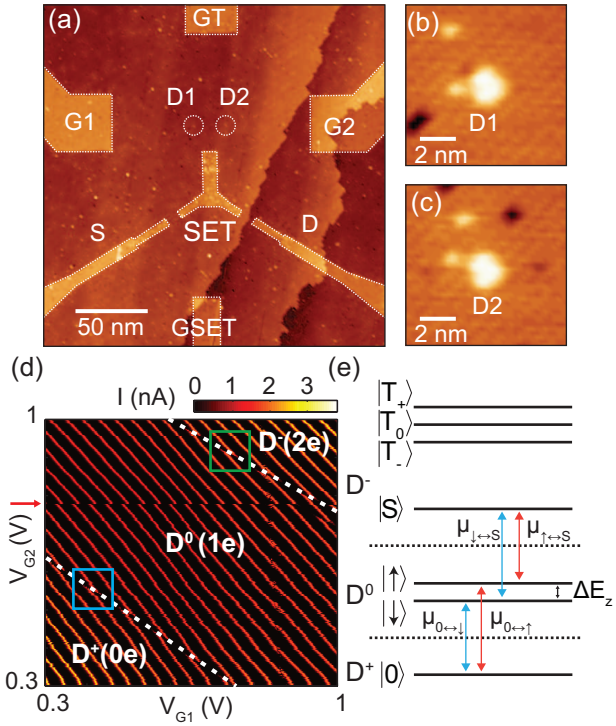

FIG. 1. **Stability diagram and energy levels of a single donor readout device.** (a) Overview STM image of the device architecture after lithography. (b-c) Two incorporation sites for donors, D1 and D2, were patterned 20 nm from the SET. (d) SET current, I_{SET}, as a function of gate voltages V_{G1} and V_{G2} for fixed $V_{GT} = V_{GSET} = 1$ V and $V_{SD} = 0.75$ mV and $B = 0.1$ T. Two parallel offset lines in the SET current (white dashed lines) are due to the charging of the donor in D2 from the D^+ to D^0 and D^0 to D^- charge states. (e) Energy levels of the D^+, D^0, and D^- charge states. Conventional readout is performed at the $D^+ \leftrightarrow D^0$ transition while fast readout is performed at the $D^0 \leftrightarrow D^-$ transition.

the start and duration of such events using 6,250 readout cycles, giving tunnel times $\tau_{\uparrow,out} = 6.5 \pm 0.8$ ms and $\tau_{\downarrow,in} = 5.1 \pm 0.3$ ms, respectively (Fig. 2(d)).

In this device these tunnel times were tailored to maximise the readout fidelity by positioning the donor with respect to the SET with the atomic precision of the STM. However, it is beneficial while performing quantum error correction and nuclear spin readout [8] to be able to tune these tunnel times to decrease the readout time. As the location of the readout position in gate-space (blue circle in Fig. 2(a)) is determined by the alignment of donor and SET electrochemical potentials there is limited electrostatic control over the tunnel rates. For more rapid spin readout and initialization, we can employ a novel pulse sequence at the two-electron $D^0 \leftrightarrow D^-$ transition (Fig. 2(e) and green box in Fig. 1(d)). Different from the D^0 charge state, the D^- is only weakly bound below the silicon conduction band edge with both electrons effectively screening the donor nucleus. Consequently, the wavefunction overlap between the D^- state and the SET island is larger resulting in faster tunnel times by nearly two orders of magnitude.

The ground state of the two-electron D^- state is a spin singlet ($|S\rangle$) with the electrochemical potentials $\mu_{\uparrow\leftrightarrow S}$ and $\mu_{\downarrow\leftrightarrow S}$ as shown in Fig. 1(e) [29]. The modified pulse sequence at this charge transition is shown in the right-hand panels of Fig. 2. The sequence is applied such that the SET current is on (off) when 1 (2) electron are bound to the donor (Fig. 2(e)). Starting with two electrons bound to the donor, we first raise both electrochemical potentials above that of the SET (Fig. 2(g)). This allows a single electron to tunnel to the SET island, leaving behind an electron of arbitrary spin orientation. This spin can subsequently be read out by aligning the electrochemical potential of the SET such that it lies between $\mu_{\uparrow\leftrightarrow S}$ and $\mu_{\downarrow\leftrightarrow S}$. If the donor-bound electron is in its $|\downarrow\rangle$ ground state then its electrochemical potential for a $|\downarrow\rangle \rightarrow |S\rangle$ transition is above that of the SET and tunnelling to the donor is prohibited (red trace in Fig. 2(f)). However, if the electron is in its $|\uparrow\rangle$ excited state, transitions $|\uparrow\rangle \rightarrow |S\rangle$ are permitted and a second electron tunnels onto the donor, forming a spin singlet. The result is a single current pulse at the start of the read phase (blue trace in Fig. 2(f)) with an electron remaining in the $|\downarrow\rangle$ ground state at the end of the pulse sequence. The current during the $D^0 \leftrightarrow D^-$ readout is greater than at the $D^+ \leftrightarrow D^0$ readout due to a decrease in the tunnel barriers towards more positive gate voltages and from a background undulation of the current through the SET from a modulated density of states in the leads (see Supplemental Material S1). Again, we estimate the readout time scale from histograms of the start and duration of the single current pulses using 22,000 readout cycles and find tunnel times $\tau_{\downarrow,in} = 140 \pm 10$ μs and $\tau_{\uparrow,out} = 130 \pm 20$ μs (Fig. 2(h)). The enhancement of qubit readout timescales by nearly two orders of magnitude highlights the advantage of readout via the D^- state.

Spin relaxation rates, $1/T_1$, have been measured using both the above pulse sequences (Fig. 2) and are determined by fitting the exponential decay of the $|\uparrow\rangle$ probability, $P_\uparrow$, as a function of wait time after loading. Values for $1/T_1$, obtained by utilizing the D^- charge state, are shown as red squares in Fig. 3 and agree perfectly with values obtained via conventional spin readout at the $D^+ \leftrightarrow D^0$ transition (black squares). However, the faster $D^0 \leftrightarrow D^-$ readout allows the spin to be measured at higher magnetic fields ($B > 5$ T) compared to the $D^+ \leftrightarrow D^0$ readout where the spin relaxes before the electron can tunnel out ($T_1 > \tau_{\uparrow,out}$). We find $1/T_1 \propto B^5$ as expected for individual P donors in silicon as spin lifetimes are limited by the valley repopulation mechanism [30–32]. Indeed, a fit obtained by Morello *et al.* [10] using a proportionality constant $K_5 = 0.015$ in a previous spin readout experiment shows excellent agreement with our data (red line in Fig. 3), independently confirming the presence of a single P donor in the device.

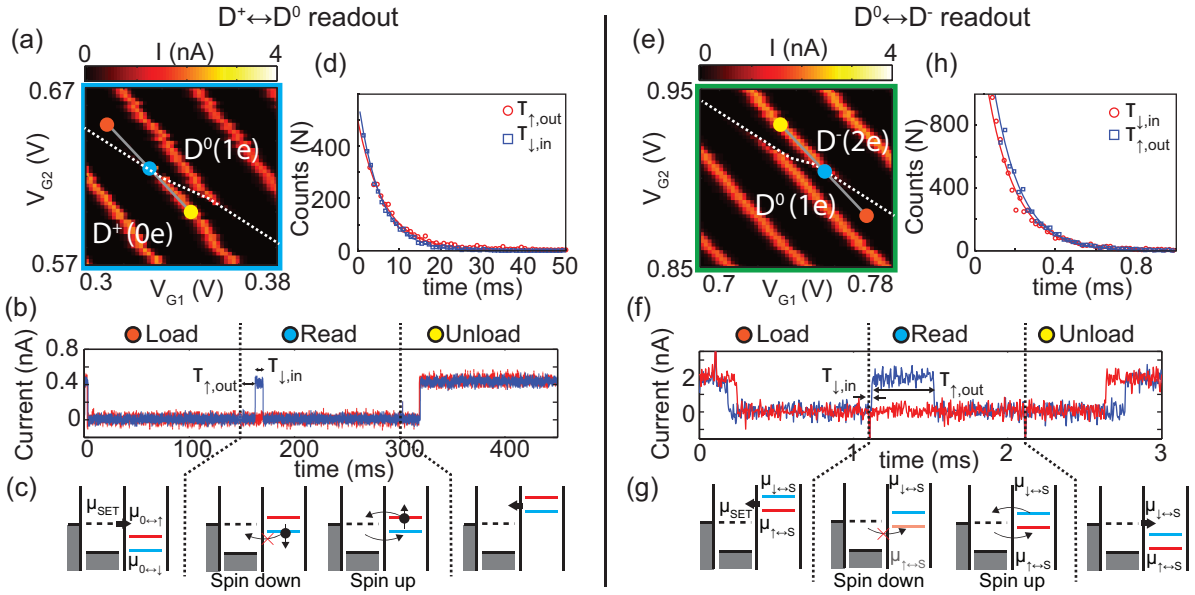

FIG. 2. $D^+ \leftrightarrow D^0$ **and** $D^0 \leftrightarrow D^-$ **single-shot spin readout.** (a,e) Close-ups of the stability diagram at the (a) $D^+ \leftrightarrow D^0$ and the (e) $D^0 \leftrightarrow D^-$ charge transitions show the position of the three level gate pulses for single-shot spin readout. (b,f) SET current response for $|\uparrow\rangle$ (blue trace) and $|\downarrow\rangle$ (red trace) during readout performed at $B = 1.6$ T and $V_{SD} = 300$ μV. (c,g) Electrochemical potentials of donor and SET during load, read, and unload phases. (d) From histograms of the start and duration of single current pulses using 6,250 $D^+ \leftrightarrow D^0$ readout cycles we extract tunnel times $\tau_{\uparrow,out} = 6.5 \pm 0.8$ ms and $\tau_{\downarrow,in} = 5.1 \pm 0.3$ ms, respectively. (h) Similarly, using 22,000 $D^0 \leftrightarrow D^-$ readout cycles we extract tunnel times $\tau_{\downarrow,in} = 140 \pm 10$ μs and $\tau_{\uparrow,out} = 130 \pm 20$ μs.

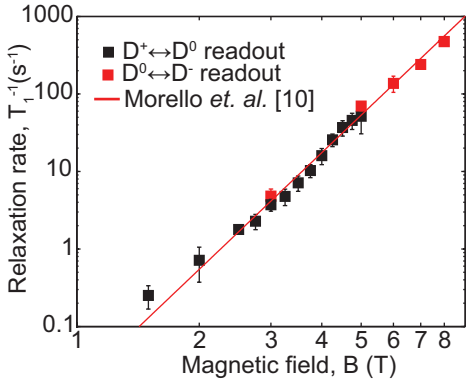

FIG. 3. **Magnetic field dependence of** T_1**.** Comparison of spin relaxation rates $T_1^{-1}(B)$ measured both using conventional readout (black squares) and readout via the D^- charge state (red squares). The solid red line shows a fit ($\propto B^5$) in agreement with Morello *et al.* for an individual P donor [10].

With faster qubit readout established, we finally need to confirm that the readout fidelity – the probability of the correct assignment of a $|\uparrow\rangle$ or $|\downarrow\rangle$ electron state after readout – is not compromised as a result of an increased measurement bandwidth and its associated noise. Using both methods, the detection of current above a threshold I_T results in the assignment of a $|\uparrow\rangle$ electron. The fidelity of this detection scheme can be estimated by numerical modelling of the distribution of the peak current, I_{peak}, during the readout phase [10] (see Supplemental Material S3). For the calculation we use 6,250 (22,000) current traces, measured during the $D^+ \leftrightarrow D^0$ ($D^0 \leftrightarrow D^-$) readout, respectively, at $B = 1.6$ T and a measurement bandwidth of 10 kHz (100 kHz). A higher bandwidth was required for the $D^0 \leftrightarrow D^-$ readout due to the faster tunnel times resulting in a lower signal to noise ratio. This magnetic field was chosen as it is a typical field used in electron and nuclear spin resonance experiments in donor-based devices [1, 33]. From the model, the electrical fidelities of the $|\uparrow\rangle$ and $|\downarrow\rangle$ spin states, $F_\uparrow$ and $F_\downarrow$, as well as the visibility, defined as $V = 1 - F_\uparrow - F_\downarrow$, can be determined as a function of threshold current and are shown in Fig. 4(a-b) for both the D^+ and D^- readout. For the values for I_T that give the maximum visibility we find $F_\uparrow = 99.6\%$ and $F_\downarrow = 100\%$ for the $D^+ \leftrightarrow D^0$ readout and $F_\uparrow = 97.6\%$ and $F_\downarrow = 99.8\%$ for the $D^0 \leftrightarrow D^-$ readout.

Importantly, a potential source of error in the measurement fidelity is the thermal broadening of the Fermi distribution in the SET ($T_e \sim 160$ mK). For the $D^+ \leftrightarrow D^0$ readout this results in a finite probability, α, for a $|\downarrow\rangle$ electron to tunnel from the donor to the SET and to be incorrectly assigned as $|\uparrow\rangle$. This can be estimated by counting tunnelling events after a time t_1 where all the $|\uparrow\rangle$ electrons have tunnelled from the donor, $t_1 \gg \tau_{\uparrow,out}$ (Fig. 4(c)). During the readout, 44 out of the 3125 ($50\% \times 6250$) $|\downarrow\rangle$ electrons tunnel from the donor between the times $t_1 = 100$ ms and $t_2 = 450$ ms. Therefore, an estimate of the tunnel time $\tau_{\downarrow,out}$ can be found by solv-

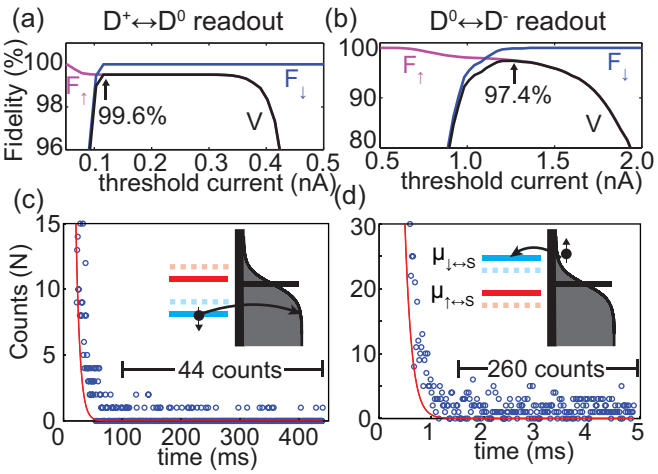

FIG. 4. **Measurement fidelities of the $D^+ \leftrightarrow D^0$ and $D^0 \leftrightarrow D^-$ readout.** Electrical fidelities ($F_\uparrow$ and $F_\downarrow$) and visibility (V) as a function of threshold current for the (a) $D^+ \leftrightarrow D^0$ and (b) $D^0 \leftrightarrow D^-$ readout. The optimal threshold current results in a visibility of $V = 99.6\%$ for the $D^+ \leftrightarrow D^0$ readout and $V = 97.4\%$ for the $D^0 \leftrightarrow D^-$ readout. (c) Histogram of the start time of the single current pulse during the $D^+ \leftrightarrow D^0$ readout. From the counts after a time $t_1 = 100$ ms where all $|\uparrow\rangle$ electrons have tunnelled from the donor we estimate the $|\downarrow\rangle$ tunnel out time to be $\tau_{\downarrow,out} = 24 \pm 4$ s. (d) From a similar histogram for the $D^0 \leftrightarrow D^-$ readout we find $\tau_{\uparrow,in} = 145 \pm 9$ ms.

ing, $\exp(\frac{-t_1}{\tau_{\downarrow,out}}) - \exp(\frac{-t_2}{\tau_{\downarrow,out}}) = (44 \pm \sqrt{44})/3125$, which gives $\tau_{\downarrow,out} = 24 \pm 4$ s. For an optimised readout time $\Delta t = 55$ ms we find $\alpha = 1 - \exp(-\frac{\Delta t}{\tau_{\downarrow,out}}) = 0.3\%$. In the experiment we significantly reduced α from $\sim 2\%$ to 0.3% by increasing $\tau_{\downarrow,out}$ through positioning the $|\downarrow\rangle$ electrochemical potential of the donor the maximum energy below the thermally broadened Fermi level of the SET while still maintaining readout (see inset of Fig. 4(c)).

This analysis is repeated for the $D^0 \leftrightarrow D^-$ readout. Here, tunnelling of a $|\uparrow\rangle$ electron to the donor now results in the incorrect assignment of a $|\downarrow\rangle$ electron. From the histogram shown in Fig. 4(d) we find $\tau_{\uparrow,in} = 145 \pm 9$ ms giving $\alpha = 0.7\%$ for an optimised readout time of $\Delta t = 1$ ms. Together with the above electrical fidelities this gives an average measurement fidelity [34] for the $D^+ \leftrightarrow D^0$ and $D^0 \leftrightarrow D^-$ spin readout of $F_M = ((1-\alpha)F_\downarrow + F_\uparrow)/2 = 99.6\%$ and $F_M = 98.4\%$, respectively. This demonstrates extremely high measurement fidelities in readout with two significantly different tunnel rates.

In addition to being able to rapidly measure the spin state of the qubit with high fidelity, the rapid initialization of a qubit into a defined state is a further key requirement for scalable quantum computing as quantum error correction requires a continuous supply of ancilla qubits which can be initialized much faster than the qubit coherence time [35]. For electron spin qubits, one method to initialize spins is to perform spin readout as described above as it naturally leaves electron spins in their $|\downarrow\rangle$ ground state. The initialisation fidelity F_I of the $D^+ \leftrightarrow D^0$ readout can be determined by modelling the occupation probability of the donor with the following rate equations,

$$\dot{p}_\downarrow(t) = -\frac{1}{\tau_{\downarrow,out}} p_\downarrow(t) + \frac{1}{\tau_{\downarrow,in}} p_0(t) + \frac{1}{T_1} p_\uparrow(t), \quad (1)$$

$$\dot{p}_\uparrow(t) = -\frac{1}{\tau_{\uparrow,out}} p_\uparrow(t) + \frac{1}{\tau_{\uparrow,in}} p_0(t) - \frac{1}{T_1} p_\uparrow(t), \quad (2)$$

where p_0 is the probability that the donor is unoccupied and $p_\downarrow(t)$ ($p_\uparrow(t)$) is the probability of the donor being occupied with a $|\downarrow\rangle$ ($|\uparrow\rangle$) spin. The sum of these probabilities is $p_0 + p_\downarrow + p_\uparrow = 1$. The $|\uparrow\rangle$ tunnel in time $\tau_{\uparrow,in} = 5.4 \pm 0.6$ ms was extracted from a histogram of the duration of the first current pulse in readout traces with multiple current pulses. Multiple pulses in the current signal are a result of a $|\uparrow\rangle$ electron tunnelling back onto the donor after a $|\uparrow\rangle$ spin has tunnelled from the donor due to thermal broadening in the SET. Solving this system of coupled differential equation with initial conditions $p_0(0) = 0\%$, $p_\downarrow(0) = 50\%$, and $p_\uparrow(0) = 50\%$, we find the $|\downarrow\rangle$ probability saturates to $F_I = p_\downarrow = 99.9\%$ after a time $t = 100$ ms. From similar rate equations for the $D^0 \leftrightarrow D^-$ readout we find $F_I = 99.8\%$ after a time $t = 3$ ms, demonstrating a method for high fidelity rapid initialisation of spin qubits.

In conclusion, we have demonstrated single shot spin readout via the D^- charge state of a precision placed single donor. With faster qubit read out by nearly two orders of magnitude, we achieve readout fidelities, $F_M = 98.4\%$, which are only marginally reduced from the measured record fidelity, $F_M = 99.6\%$, using conventional spin readout. Furthermore, the D^- readout is a fast method for high fidelity ($F_I = 99.8\%$) qubit initialisation. This number is above the threshold of error correction protocols such as the surface code and may further be improved through efforts to lower the electron temperature and reduce measurement noise.

This research was conducted by the Australian Research Council Centre of Excellence for Quantum Computation and Communication Technology (Project Number CE110001027) and the U.S. National Security Agency and the U.S. Army Research Office under Contract Number W911NF-08-1-0527. M.Y.S. acknowledges an ARC Laureate Fellowship.

* Present address: School of Physics and Astronomy, Monash University, Melbourne, VIC 3800, Australia
† Present address: Center for Nanotechnology Innovation @ NEST, Istituto Italiano di Tecnologia, Piazza San Silvestro 12, 56127 Pisa, Italy
‡ michelle.simmons@unsw.edu.au

[1] J. T. Muhonen, J. P. Dehollain, A. Laucht, F. E. Hudson, R. Kalra, T. Sekiguchi, K. M. Itoh, D. N. Jamieson, J. C. McCallum, A. S. Dzurak, and A. Morello, Nat. Nano. **9**, 986 (2014).

[2] M. Veldhorst, J. J. C. Hwang, C. H. Yang, A. W. Leenstra, B. de Ronde, J. P. Dehollain, J. T. Muhonen, F. E. Hudson, K. M. Itoh, A. Morello, and A. S. Dzurak, Nat. Nano. **9**, 981 (2014).

[3] J. R. Petta, A. C. Johnson, J. M. Taylor, E. A. Laird, A. Yacoby, M. D. Lukin, C. M. Marcus, M. P. Hanson, and A. C. Gossard, Science **309**, 2180 (2005).

[4] R. Kalra, A. Laucht, C. D. Hill, and A. Morello, Phys. Rev. X **4**, 021044 (2014).

[5] L. C. L. Hollenberg, A. D. Greentree, A. G. Fowler, and C. J. Wellard, Phys. Rev. B **74**, 045311 (2006).

[6] J. M. Taylor, H. A. Engel, W. Dur, A. Yacoby, C. M. Marcus, P. Zoller, and M. D. Lukin, Nat. Phys. **1**, 177 (2005).

[7] M. Steger, K. Saeedi, M. L. W. Thewalt, J. J. L. Morton, H. Riemann, N. V. Abrosimov, P. Becker, and H.-J. Pohl, Science **336**, 1280 (2012).

[8] J. J. Pla, K. Y. Tan, J. P. Dehollain, W. H. Lim, J. J. L. Morton, F. A. Zwanenburg, D. N. Jamieson, A. S. Dzurak, and A. Morello, Nature **496**, 334 (2013).

[9] J. M. Elzerman, R. Hanson, L. H. Willems van Beveren, B. Witkamp, L. M. K. Vandersypen, and L. P. Kouwenhoven, Nature **430**, 431 (2004).

[10] A. Morello, J. J. Pla, F. A. Zwanenburg, K. W. Chan, K. Y. Tan, H. Huebl, M. Mottonen, C. D. Nugroho, C. Yang, J. A. van Donkelaar, A. D. C. Alves, D. N. Jamieson, C. C. Escott, L. C. L. Hollenberg, R. G. Clark, and A. S. Dzurak, Nature **467**, 687 (2010).

[11] H. Büch, S. Mahapatra, R. Rahman, A. Morello, and M. Y. Simmons, Nat. Commun. **4**, (2013).

[12] E. Kawakami, P. Scarlino, D. R. Ward, F. R. Braakman, D. E. Savage, M. G. Lagally, M. Friesen, S. N. Coppersmith, M. A. Eriksson, and L. M. K. Vandersypen, Nat. Nano. **9**, 666 (2014).

[13] R. Raussendorf and J. Harrington, Phys. Rev. Lett. **98**, 190504 (2007).

[14] A. G. Fowler, M. Mariantoni, J. M. Martinis, and A. N. Cleland, Phys. Rev. A **86**, 032324 (2012).

[15] B. Weber, S. Mahapatra, T. F. Watson, and M. Y. Simmons, Nano Lett. **12**, 4001 (2012).

[16] B. Weber, T. H. Matthias, S. Mahapatra, T. F. Watson, H. Ryu, R. Rahman, H. C. L., G. Klimeck, and M. Y. Simmons, Nat. Nano. **9**, 430 (2014).

[17] T. F. Watson, B. Weber, J. A. Miwa, S. Mahapatra, R. M. P. Heijnen, and M. Y. Simmons, Nano Lett. **14**, 1830 (2014).

[18] H. Sellier, G. P. Lansbergen, J. Caro, S. Rogge, N. Collaert, I. Ferain, M. Jurczak, and S. Biesemans, Phys. Rev. Lett. **97**, 206805 (2006).

[19] M. Pierre, R. Wacquez, X. Jehl, M. Sanquer, M. Vinet, and O. Cueto, Nat. Nano. **5**, 133 (2010).

[20] A. Fuhrer, M. Fuechsle, T. C. G. Reusch, B. Weber, and M. Y. Simmons, Nano Lett. **9**, 707 (2009).

[21] B. Weber, S. Mahapatra, H. Ryu, S. Lee, A. Fuhrer, T. C. G. Reusch, D. L. Thompson, W. C. T. Lee, G. Klimeck, L. C. L. Hollenberg, and M. Y. Simmons, Science **335**, 64 (2012).

[22] B. Weber, H. Ryu, Y.-H. M. Tan, G. Klimeck, and M. Y. Simmons, Phys. Rev. Lett. **113**, 246802 (2014).

[23] S. R. McKibbin, W. R. Clarke, A. Fuhrer, T. C. G. Reusch, and M. Y. Simmons, Appl. Phys. Lett. **95**, 233111 (2009).

[24] M. Fuechsle, J. A. Miwa, S. Mahapatra, H. Ryu, S. Lee, O. Warschkow, L. C. L. Hollenberg, G. Klimeck, and M. Y. Simmons, Nat. Nano. **7**, 242 (2012).

[25] See Supplemental Material [URL], which includes Refs. [10, 11, 15, 20, 36].

[26] S. Mahapatra, H. Büch, and M. Y. Simmons, *Nano Letters*, Nano Lett. **11**, 4376 (2011).

[27] A. K. Ramdas and S. Rodriguez, Rep. Prog. Phys. **44**, 1297 (1981).

[28] R. Hanson, L. P. Kouwenhoven, J. R. Petta, S. Tarucha, and L. M. K. Vandersypen, Rev. Mod. Phys. **79**, 1217 (2007).

[29] The corresponding triplet excited states, T_-, T_0 and T_+, are considered inaccessibly high in energy due to their large exchange splitting from the S ground state ($\sim$meV) and will not be considered in any subsequent discussion.

[30] H. Hasegawa, Phys. Rev. **118**, 1523 (1960).

[31] D. K. Wilson and G. Feher, Phys. Rev. **124**, 1068 (1961).

[32] F. A. Zwanenburg, A. S. Dzurak, A. Morello, M. Y. Simmons, L. C. L. Hollenberg, G. Klimeck, S. Rogge, S. N. Coppersmith, and M. A. Eriksson, Rev. Mod. Phys. **85**, 961 (2013).

[33] A. Laucht, J. T. Muhonen, F. A. Mohiyaddin, R. Kalra, J. P. Dehollain, S. Freer, F. E. Hudson, M. Veldhorst, R. Rahman, G. Klimeck, K. M. Itoh, D. N. Jamieson, J. C. McCallum, A. S. Dzurak, and A. Morello, Sci. Adv. **1**, e1500022 (2015).

[34] J. J. Pla, K. Y. Tan, J. P. Dehollain, W. H. Lim, J. J. L. Morton, D. N. Jamieson, A. S. Dzurak, and A. Morello, Nature **489**, 541 (2012).

[35] D. P. DiVincenzo, Fortschr. Phys. **48**, 771 (2000).

[36] K. Nabors and J. White, IEEE Trans. Comput.-Aided Des. Integr. Circuits Syst. **10**, 1447 (1991).